Passive Radio Frequency Beamformer Using Transmission-Line Transformers And Tunable Capacitors

Matthew Anderson
Ali Niknejad
Jan M. Rabaey

Electrical Engineering and Computer Sciences
University of California, Berkeley

Technical Report No. UCB/EECS-2023-50
http://www2.eecs.berkeley.edu/Pubs/TechRpts/2023/EECS-2023-50.html

May 1, 2023

Passive Radio Frequency Beamformer Using Transmission-Line Transformers And Tunable Capacitors

by

Matthew Giorgis Anderson

A thesis submitted in partial satisfaction of the

requirements for the degree of

Masters of Science, Plan II

in

Electrical Engineering and Computer Science

in the

Graduate Division

of the

University of California, Berkeley

Committee in charge:

Professor Jan M. Rabaey, Chair
Professor Ali M. Niknejad
Professor Martin White

Spring 2022

The thesis of Matthew Giorgis Anderson, titled Passive Radio Frequency Beamformer Using Transmission-Line Transformers And Tunable Capacitors, is approved:

Chair _____ Date _____

_____ Date _____

_____ Date _____

University of California, Berkeley

Passive Radio Frequency Beamformer Using Transmission-Line Transformers And Tunable Capacitors

Abstract

Passive Radio Frequency Beamformer Using Transmission-Line Transformers And Tunable Capacitors

by

Matthew Giorgis Anderson

Masters of Science, Plan II in Electrical Engineering and Computer Science

University of California, Berkeley

Professor Jan M. Rabaey, Chair

Traditional methods for RF beamforming require significant amounts of power, making them difficult to deploy in some low-power applications. A simple, fully-passive, low-loss technique for Radio Frequency (RF) beamforming is realized by serially combining the antennas in an array using transmission-line transformers (without magnetic components) incorporated into the feed line and a programmable admittance placed in shunt across each antenna's feed port. Utilizing the feed structure for signal combining eliminates the need for additional RF combining structures. Further, taking advantage of the symmetry inherent in a phased array, we propose a new method for passive phase shifting that only requires one tunable element per antenna. The proposed fully-passive beamformer is demonstrated on an FR4 printed circuit board with a linear, two-element, array of half-wave dipoles at 2.05 GHz using a digitally tunable capacitor as the programmable admittance. A loss in array gain of 1.07 dB is realized when compared to an identical array with ideal phase combining.

To A Better Future

...

Contents

List of Figures

List of Tables

Acknowledgments

I wish to acknowledge the contributions of the students, faculty and sponsors of Berkeley Wireless Research Center as well as the support of my loving family.

Chapter 1

Introduction

1.1 Motivation

Phased arrays [1] have become increasingly important in recent years as wireless networks utilize higher frequencies to alleviate over crowding and increase bandwidth. In this context, phased arrays provide significant benefits by allowing the nodes within a wireless network to quickly steer their beams to maximize signal strength and reduce overall interference. Fig. 1.1 shows some current applications for phased arrays.

That said, there are pressing power challenges to implementing phase arrays in modern wireless networks [2, 3, 4]. These systems require many antenna elements, each with their

Figure 1.1: Examples of applications using phased arrays.

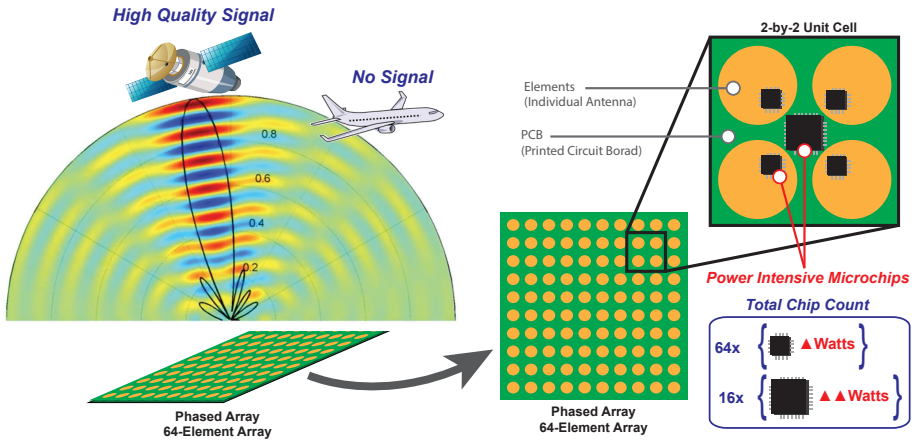

Figure 1.2: Illustration of phased array function and resulting large power consumption.

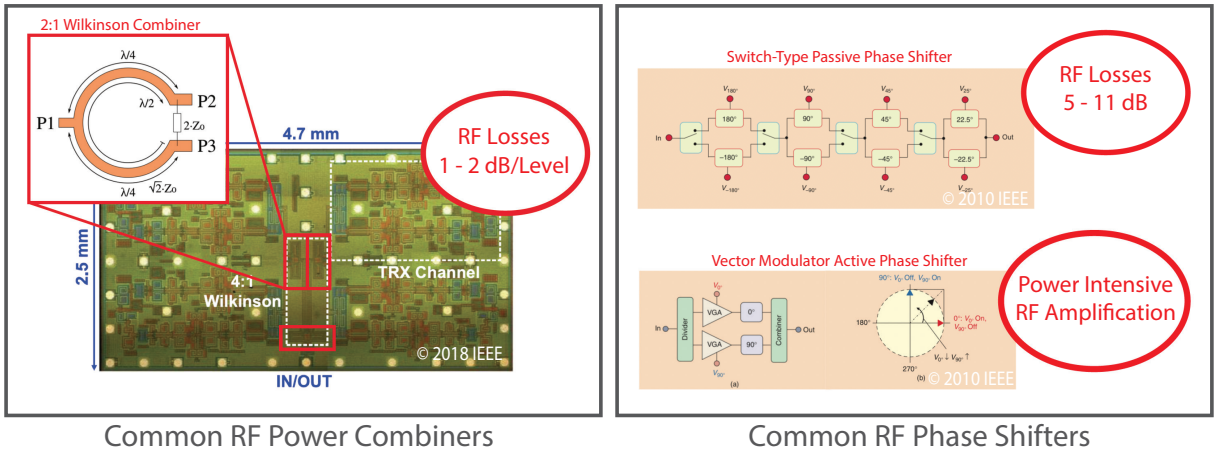

Figure 1.3: Popular techniques for power combining and phase shifting in literature [5, 6].

own power-hungry radio frequency (RF) signal chains and signal processing. The result being, a significant increase in RF power consumption for phased array beamforming systems when compared to omni-directional wireless systems at lower frequencies. Even in modestly sized arrays, this added power consumption can be problematic for both battery-life and thermal management. Fig. 1.2 illustrates how phased arrays use constructive interference between the signals from multiple antenna to steer a wireless beam and how the many chips required to process these signals result in large power consumption. This operation of precise phase shifting and summation to form the wireless beams is called beamforming. Existing techniques for beamforming [5, 6] generally require significant power or are very lossy, see examples in Fig. 1.3.

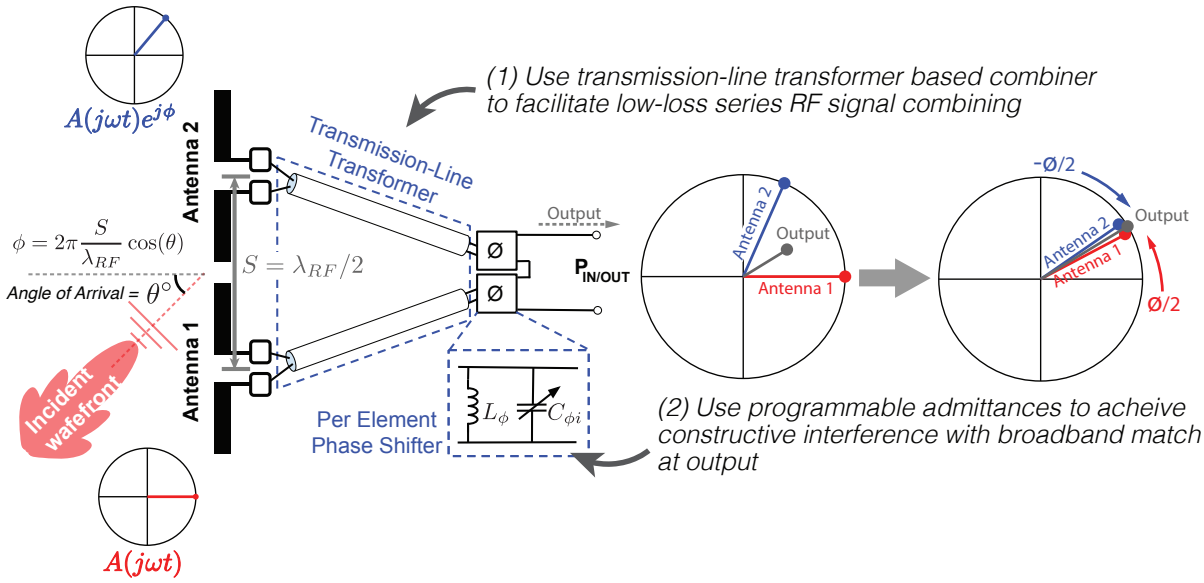

Figure 1.4: Proposed two-element series connected array with low-loss passive beamformer.

To address this, a technique for performing radio frequency (RF) phase shifting and summation with very low loss and zero active power consumption is presented here. To our knowledge, this is the first demonstration of a phased array utilizing transmission-line transformers (TLTs) [7] incorporated into the feed lines and balanced passive impedance tuning to construct an RF beamforming phased array. Utilizing the feed structure for signal combining eliminates the need for additional lossy RF combining structures and the use of balanced passive impedance tuning reduces the complexity associated with phase shifting. Altogether this allows for the realization of a simple, low power and low loss RF beamformer at microwave frequencies. An example system is shown in Fig. 1.4 and is explained in more detail in the following sections.

1.2 Thesis Organization

In Chapter 2, the theory and workings of the proposed low-loss passive beamformer are described, including a description of power-combining using TLTs and the principle for balanced impedance tuning. In Chapter 3, the prototype design is detailed. The realization of the TLT, phase shifters and antenna elements is highlighted as well as the design of a reference board for comparison. Chapter 4 reports the experimental setup, simulation environment, and measurement results obtained using the prototype array. Chapter 5 concludes this work.

Chapter 2

Theory

There are two major components which enable this form of fully-passive RF beamforming. The first is transmission-line transformers (TLTs) built into the RF feed lines, which serve to condition the signals from each antenna element for simple low-loss series combining in the RF-domain. The second is balanced impedance tuning of passives for phase shifting, which utilize array symmetry to reduce component counts and realize a basic low-loss phase shifter. Each of these are described briefly below. Note, the analysis that follows is for the receive configuration but holds for transmit as well, since the structures are all passive and reciprocal.

2.1 Power-Combining with Transmission-Line Transformers (TLTs)

TLTs have been used for impedance transformation for many years [7, 8]. More recently, series voltage combining using TLTs has been proposed in the design of high power output RF power amplifiers [8]. However, in this work they serve to transform the effective common-mode impedance of each antenna to a large magnitude value, enabling simple series connections for power combining. To my knowledge, the use of a TLT to combine signals from multiple antennas in a phased array has not been done before.

Physically separated RF antennas require transmission (or feed) lines to route signals to a centralized location for processing. In the case of balanced antennas, with minimal modification these feed lines can also implement a TLT that can be used for low-loss signal combining in the RF domain. An example is shown in Fig. 2.1a, where 2 in-phase differential antennas ('Source 1' and 'Source 2'), with the same differential source resistance (R_S), common mode impedance (Z_{CM}) and output voltage (V_S), are connected in series to a load ($R_L = 2 \times R_S$) through differential feed lines. If the differential characteristic impedance of the feed lines ($Z_{o(DM)}$) is set to R_S, it can be shown that the circuit in Fig. 2.1a is transformed into Fig. 2.1b. Note that the effective differential source resistance is unchanged. But the common mode source resistance (Z_{CM}) is transformed to an effective common mode

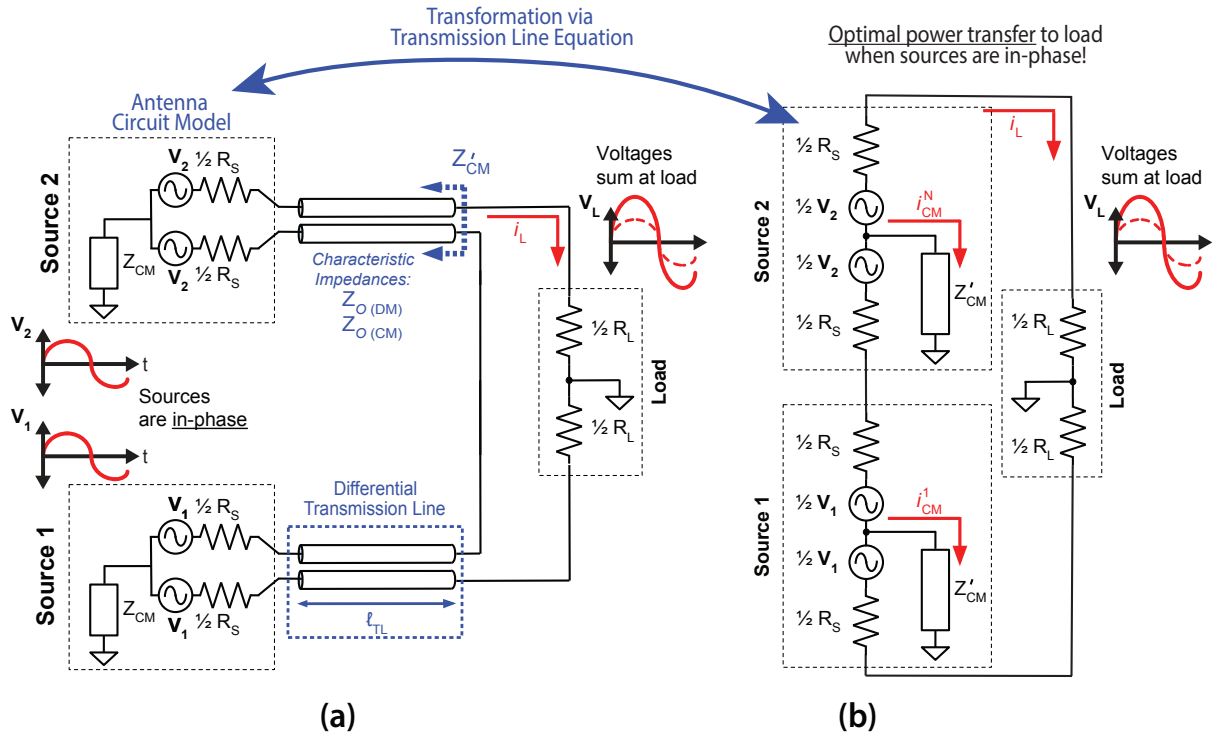

Figure 2.1: Transformation of series-connected phased array circuit model using transmission line equation.

source resistance (Z'_{CM}), where Z'_{CM} is described by the transmission line equation shown in Eq. 2.1. The value of Z'_{CM} is a function of the length of the feed lines (l_{TL}), the common-mode characteristic impedance of the feed lines ($Z_{o(CM)}$) and Z_{CM}.

$$Z'_{CM} = Z_{o(CM)} \frac{Z_{CM} + jZ_{o(CM)} tan\left(2\pi \frac{\ell_{TL}}{\lambda_{RF}}\right)}{Z_{o(CM)} + jZ_{CM} tan\left(2\pi \frac{\ell_{TL}}{\lambda_{RF}}\right)} \tag{2.1}$$

From the circuit in Fig. 2.1b and Eq. 2.2 and 2.3, we can show in the case of boadside incident waves (in-phase sources), the series connected antennas in this array optimally transfer all their available power (P_{AVS}) to the load ($P_L = NP_{AVS}$), provided Z'_{CM} is large.

$$Let: \; R_L = 2R_S, \; P_{AVS} = \frac{V_S^2}{8R_S}, \; P_L = \frac{1}{2}\frac{V_L^2}{R_L} \tag{2.2}$$

$$P_L = \frac{1}{2}\left(2V_S \frac{2R_S}{4R_S}\right)^2 \frac{1}{2R_S} = 2\frac{V_S^2}{8R_S} = 2P_{AVS} \tag{2.3}$$

The primary loss mechanism for this circuit is the flow of current through Z'_{CM}, bypassing the load. From Eq. 2.1, we see that by maximizing $Z_{o(CM)}$, then selecting l_{TL} and Z_{CM} appropriately, Z'_{CM} can be made large relative to R_S, thus minimizing losses in the TLT. A quantitative derivation of the loss due to finite Z'_{CM} (and its relationship to the number of series connected elements) is beyond the scope of this work but would be a necessary area for future research if this technique is to be optimized.

2.2 Phase Shifting with Balanced Impedance Tuning

When using a TLT power combiner as described in Section 2.1, if the relative phase relationship between the antenna signals (ϕ) is non-zero, the power transfer is not optimal and is proportional to $cos^2(\phi/2)$. In effect, the TLT combiner creates a directive array and a means to steer the beam is needed. Conventional phase shifters [6] can be used to address this issue by adding the appropriate phase shift to the differential signals before they are combined. However, these phase shifters are generally either passive and quite lossy [9, 10, 11] or power-intensive [5].

In contrast, by adding a reactance in shunt across each source, as shown in Fig. 2.2, and tuning the values in a balanced way (i.e. an increase in reactance across one source is matched by decreases in reactance across another source), we can achieve near optimum power transfer over a broad range of ϕ with minimal loss and no active devices. This allows us to realize a $\pm 90^\circ$ phase shift with much fewer lossy components than a standard switch-type phase shifter.

This method of phase shifting, utilizing balanced impedance tuning, differs significantly from high/low pass and switched transmission line techniques for passive phase shifting [3,4]. By taking advantage of the symmetry inherent in a phased array, i.e. the desired phase shift on one antenna element is the negative of the desired phase shift on another, we are able to reduce the number of switchable or tunable passive components required from three or four per antenna to one, while still maintaining a good match to the load. This is because the reactance added in shunt across Source 1 is cancelled by the negative reactance added in shunt across Source 2. Reducing the number of switched or tuned elements is very important for minimizing phase shifter loss. Balanced impedance tuning as a method of phase shifting may not be limited to two-element arrays and scaling up these techniques for larger arrays would be an important area for future research. Such discussions are beyond the scope of this work.

Steering the array's beam using BIPS requires a mathematical understanding of the power received (or transmitted) under various phaseshifter configurations. This can be derived using nodal analysis, allowing us to steer the beam so as to maximize the signal from sources of interest and is discussed in the following section.

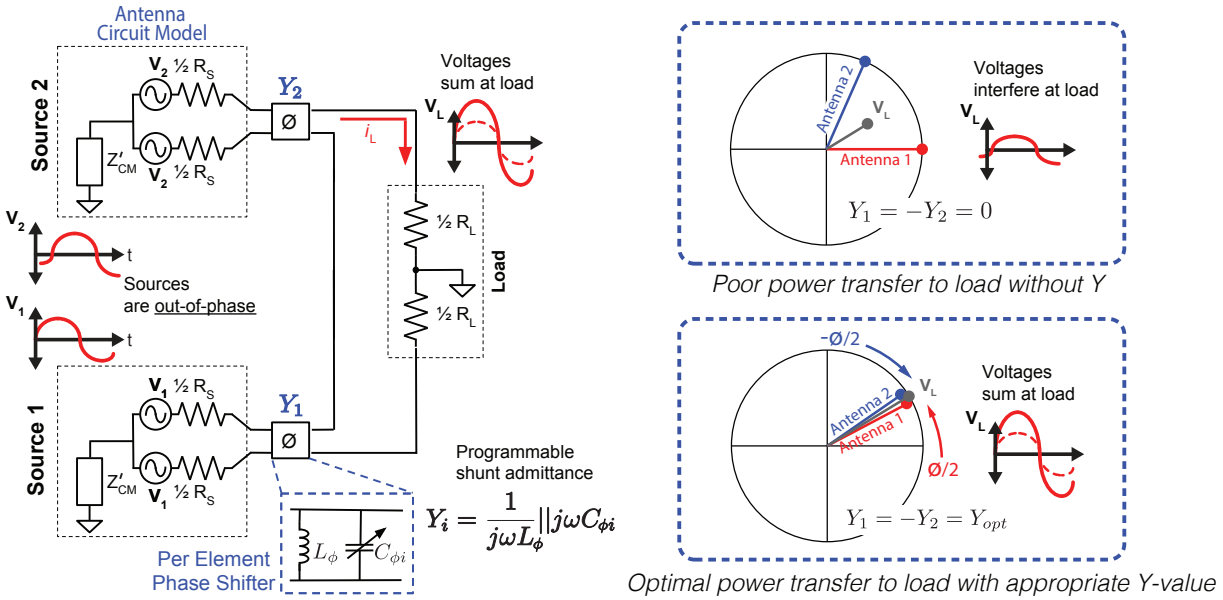

Figure 2.2: Two-element series connected array with proposed low-loss balanced-impedance-tuning phase shifter.

Deriving P_L Under Balanced Impedance Tuning Approach

For a 2-element array we can represent the circuit as shown in Fig. 2.3. To make the math more tractable we replace the sources with their Norton equivalent and assume infinite Z'_{CM}. The exact equation for the power delivered to the load (P_L) as a function of the power available from each source (P_{AVS}), the phase difference (ϕ), and the reactance across each source (Z_ϕ, where $Z_\phi = 1/Y_\phi$) is derived below.

Defining $\boldsymbol{i_L^1}$ as the load current ($\boldsymbol{i_L}$) when only $\boldsymbol{i_S^1}$ is connected and $\boldsymbol{i_L^2}$ as $\boldsymbol{i_L}$ when only $\boldsymbol{i_S^2}$ is connected. We can express $\boldsymbol{i_L^1}$ and $\boldsymbol{i_L^2}$ as a function of the known elements in the circuit and define $\boldsymbol{i_L}$ as the sum of $\boldsymbol{i_L^1}$ and $\boldsymbol{i_L^2}$ via superposition. (Note, $R_L = 2R_S$. Also note, these simplifications assume a purely reactive Z_ϕ.)

$$\boldsymbol{i_L^1} = \boldsymbol{i_S^1}\frac{R_S||-Z_\phi}{(R_S||-Z_\phi)+(R_S||+Z_\phi)+2R_S} \tag{2.4}$$

$$\boldsymbol{i_L^2} = \boldsymbol{i_S^2}\frac{R_S||+Z_\phi}{(R_S||+Z_\phi)+(R_S||-Z_\phi)+2R_S} \tag{2.5}$$

Where,

$$\frac{R_S||\pm Z_\phi}{(R_S||+Z_\phi)+(R_S||-Z_\phi)+2R_S} = \frac{|Z_\phi|^2 \pm jR_S|Z_\phi|}{4|Z_\phi|^2+2R_S^2}. \tag{2.6}$$

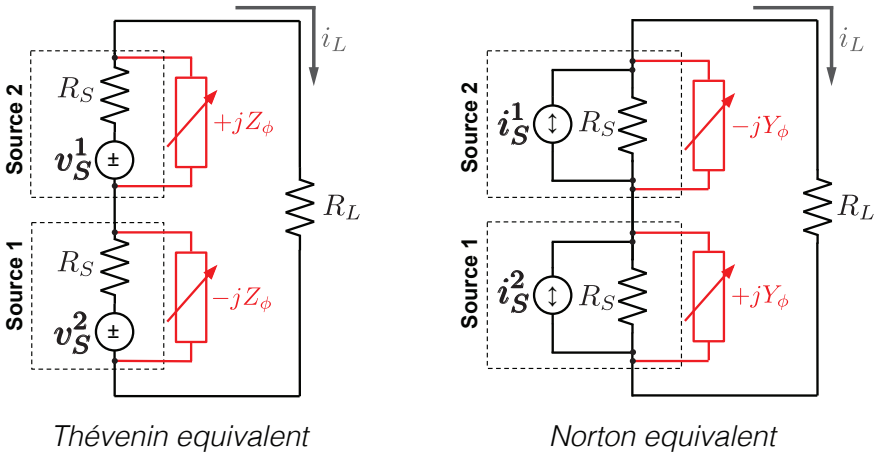

Figure 2.3: Thévenin and Norton equivalent circuit representation for balanced impedance tuning approach to phase shifting.

We can also express $\boldsymbol{i_{S1}}$ and $\boldsymbol{i_{S2}}$ in complex form as a function of P_{AVS}, R_S and ϕ.

$$\boldsymbol{i_S^1} = 2\sqrt{\frac{2P_{AVS}}{R_s}}\left[\cos(\frac{\phi}{2}) + j\sin(\frac{\phi}{2})\right] \tag{2.7}$$

$$\boldsymbol{i_S^2} = 2\sqrt{\frac{2P_{AVS}}{R_s}}\left[\cos(\frac{\phi}{2}) - j\sin(\frac{\phi}{2})\right] \tag{2.8}$$

Putting these together we find an expression for i_L and therefore P_L.

$$i_L = 4\sqrt{\frac{2P_{AVS}}{R_s}}\left[\frac{|Z_\phi|^2\cos(\frac{\phi}{2}) + |Z_\phi|R_S\sin(\frac{\phi}{2})}{4|Z_\phi|^2 + 2R_S^2}\right] \tag{2.9}$$

$$P_L = \frac{1}{2}|i_L|^2 R_L, R_L = 2R_S \tag{2.10}$$

$$P_L = 2P_{AVS}\left[\frac{|Z_\phi|^2\cos(\frac{\phi}{2}) + |Z_\phi|R_S\sin(\frac{\phi}{2})}{|Z_\phi|^2 + \frac{1}{2}R_S^2}\right]^2 \tag{2.11}$$

Multiplying the numerator and denominator by $1/(Z_\phi)^2$ and replacing the impedances with their associated admittances, we obtain:

$$P_L = 2P_{AVS}\left[\frac{\cos(\phi/2) + (Y_\phi/Y_S)\sin(\phi/2)}{1 + \frac{1}{2}(Y_\phi/Y_S)^2}\right]^2. \tag{2.12}$$

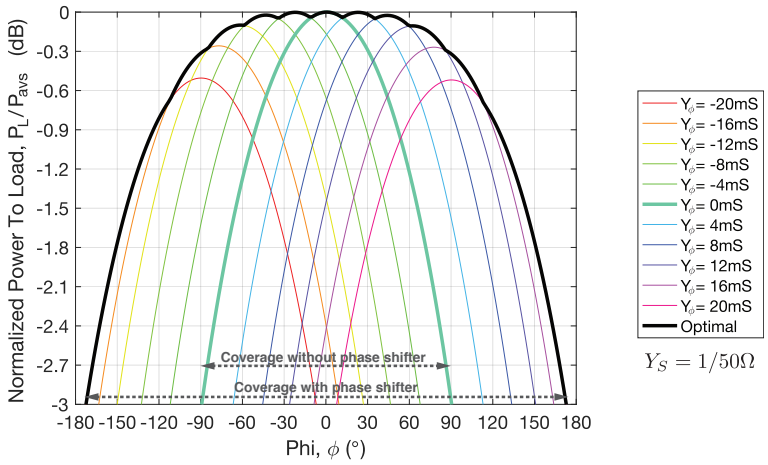

Figure 2.4: Normalized power delivered to the load over phase angle for range of admittances.

The power delivered to the load (P_L) is described by Eq. (2.12), where P_{AVS} is the power available from each source. The results from this equation are plotted in Fig. 2.4 for various Y_ϕ values, showing near optimal power transfer over a broad range of ϕ.

The efficiency of this phase shifting modality will decrease if we relax our initial assumption that Y_ϕ is purely reactive. A detailed treatment of how resistive components (or finite component Q) in Y_ϕ drive loss in the phase shifter is beyond the scope of this work but is also an important avenue for future research.

Chapter 3

Array Design

To evaluate the techniques introduced in Section 2, a prototype array was designed and fabricated using the TLT-based power combiner and balanced impedance phase shifter from off-the-shelf components. Additionally, an identical array was designed with an optimal combining technique that utilized post-processing for beamforming for comparison. Details of the two designs and their key components are presented below.

3.1 Key Components

The arrays consisted of three primary components: (1) the antennas or radiating elements, (2) RF feed lines which double as the transmission-line transformer, and (3) in the proposed array, the phase shifters based on balanced-impedance tuning.

Antennas

A two-element linear antenna array was designed. It consisted of two 2.05-GHz half-wavelength dipoles, with 75 mm (or approximately half-wavelength) spacing, arranged to maximize broadside radiation and minimize antenna interaction. Dipoles were chosen for their simplicity and because they have a balanced output which makes interface with the TLTs straight forward. The array is designed on a standard FR4 material (Isola FR370HR) with a relative dielectric constant of roughly 4.1 at 2 GHz and thickness of 1.6 mm. This resulted in dipoles of length 54.0 mm and width 5.0 mm. A series capacitance of 3.5 pF is used to match the antennas' differential impedance to 50 Ω and each matched dipole antenna was fed via a roughly one wavelength long differential microstrip feed line. A dimensioned detail of the dipole antenna is shown in Fig. 3.1.

RF Feed Lines and Transmission-Line Transformers

The length of the feed line and width of its ground plane was optimized to maximize the antenna's effective common-mode impedance while still being long enough to route around

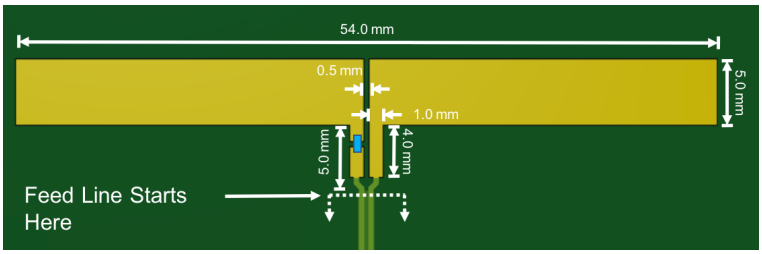

Figure 3.1: Dimensioned detail of dipole antenna with matching cap (blue).

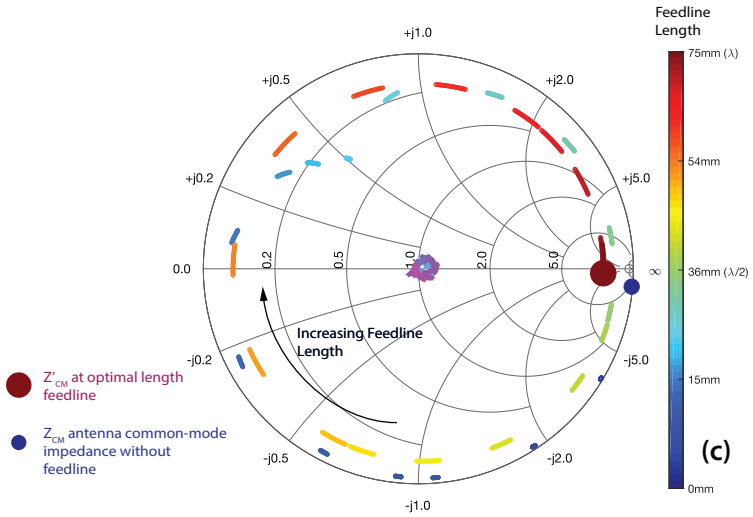

Figure 3.2: Smith chart showing effect of varying the feed line length on the effective differential (center) and common-mode (edge) antenna impedance seen at the summing node.

surface mount type (SMT) components and to the feed port(s). A Smith chart illustrating the simulated effect of extending the feed line length on the effective antenna differential and common-mode impedances is presented in Fig. 3.2. As the feed line length changes the differential impedance is virtually unchanged, while the common-mode impedance rotates around the Smith chart. The optimal electrical length for the feed lines is therefore chosen to maximize this effective common-mode impedance at f_{RF}. For this prototype, it results in a 73.4 mm long microstrip line of 462 μm trace width (W), 249 μm trace spacing (S), 1270 μm ground plane width (W_{GND}) and 89 μm separation between the ground plane and the signal traces (G). A CAD model of the PCB showing the RF feedlines is shown in Fig. 3.3.

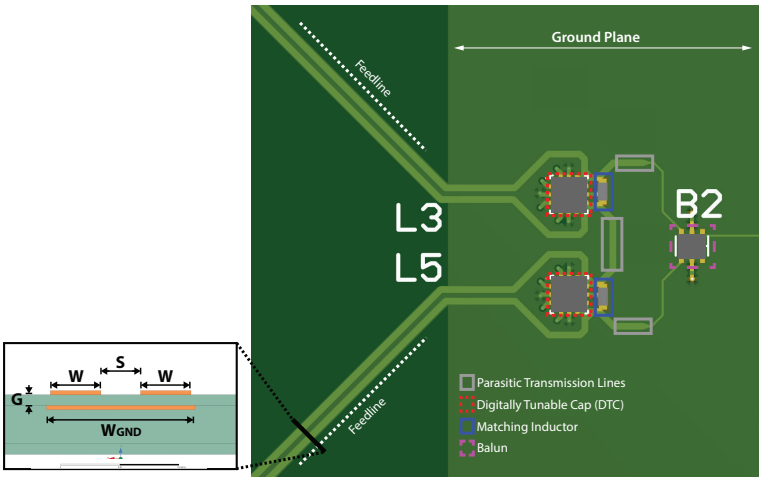

Figure 3.3: Detail of the PCB highlighting transmission-line transformers and discrete components that make up the per-element phase shifters.

Balanced Impedance Phase Shifters

The programmable admittance required for beam steering is connected in shunt across the feed port of the transmission lines driving each antenna, see Fig. 3.3. This configurable admittance is composed of a 1.6 nH fixed SMT inductor and a digitally tunable capacitor (DTC) by Peregrine Semiconductor, PE64102MLAA-Z. The DTC varies from 1.88 pF to 14.0 pF and is controlled via SPI. The values for the inductor and DTC were chosen to ensure an adequate range of Y_ϕ to maximize the range of achievable beam angles, based on Eq. 2.12. An instance of programmable admittance is connected in shunt across the end of the feed lines for each antenna.

3.2 System

After the programmable admittance, the transmission lines from each antenna are connected in series and the remaining terminals become the array's output port. The design is illustrated in Fig. 3.4. Finally, the output port is connected to a balun to map the array's differential output to a single-ended signal compatible with test equipment.

To compare the series phased array (described above), an optimal phased array is fabricated and tested – using the same antennas, antenna spacing and transmission line layout as the series phased array but without the shunt programmable admittances or the series connected feed line termination. See Fig. 3.5. Each antenna in the optimal phased array is connected to its own SMA connector and the beam steering was done in post process. Since each antenna has an independent input/output port with perfect digital phase control and signal combining, this array represents the optimal performance for the phased array.

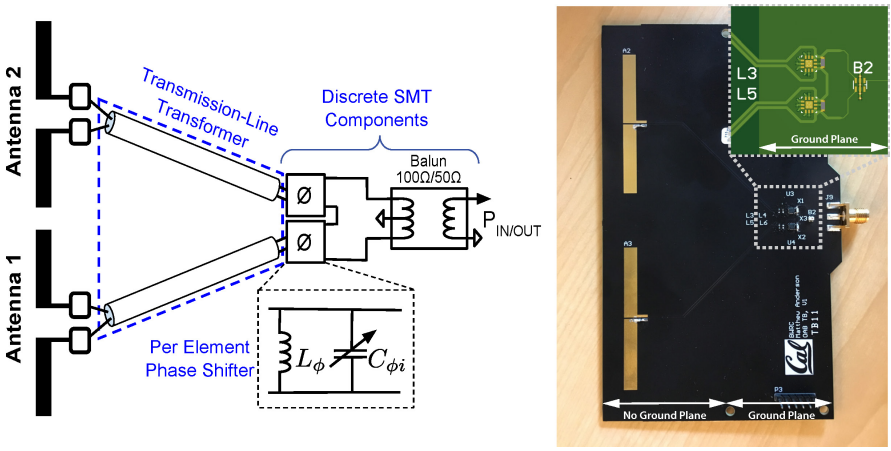

Figure 3.4: Schematic and fabricated printed circuit board for series connected or proposed antenna array with inset of transmission-line transformer summing node.

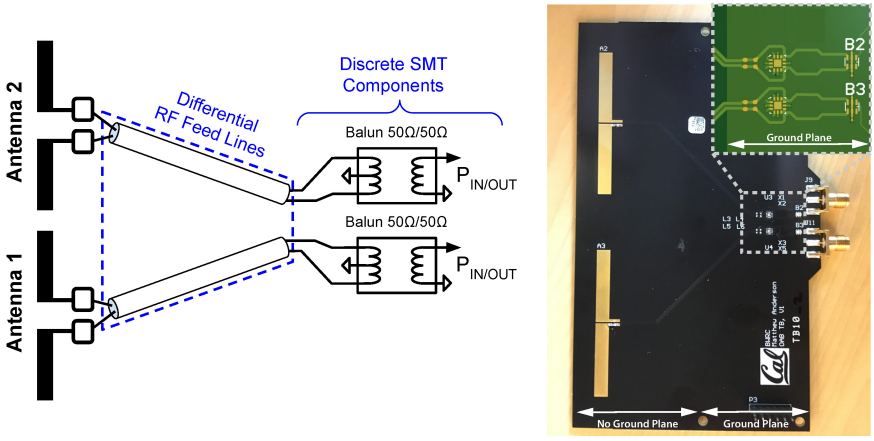

Figure 3.5: Schematic and fabricated printed circuit board for reference or optimal antenna array with individual SMA connectors for each antenna.

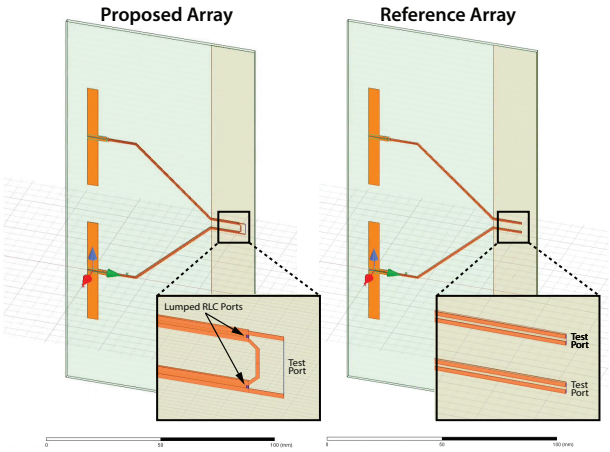

Figure 3.6: HFSS models for proposed and optimal phased array

3.3 Simulation

The beamformer designs from Section 3.2 were optimized and verified using Finite Element Method (FEM) simulations in ANSYS HFSS. The HFSS models include an identical optimal phased array and series phased array with the required configurable passives for beam steering, as illustrated in Fig. 3.6. The proposed array has lumped ports modelling shunt phase shifters, a copper trace facilitating the series connection, and a single measurement port. While the optimal phased array has individual ports for each antenna element.

Chapter 4

Measurement Results

4.1 Experimental Setup

The experimental setup used for evaluating the performance of the series phased array and reference array is shown in Fig. 4.1. It consisted of an anechoic environment (built using foam RF-absorbers), a 4-port programmable network analyzer or PNA (Agilent N5242A), two precision rotating platforms, and a USB-to-SPI adapter for digital control of the programmable admittance. This setup allows for measurement of S-parameters and array gain in azimuth angle, θ. All measurements were taken at a distance of 47.2 cm to ensure far-field operation, based on the estimated far-field distance [12] for the array.

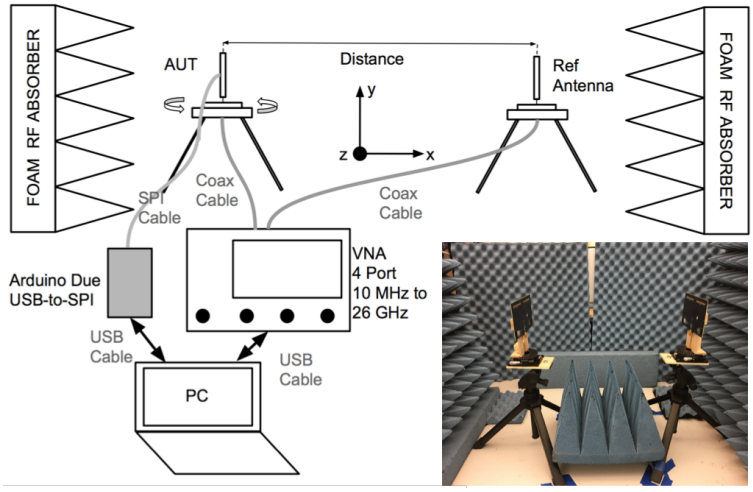

Figure 4.1: Experimental set up for far field gain characterization.

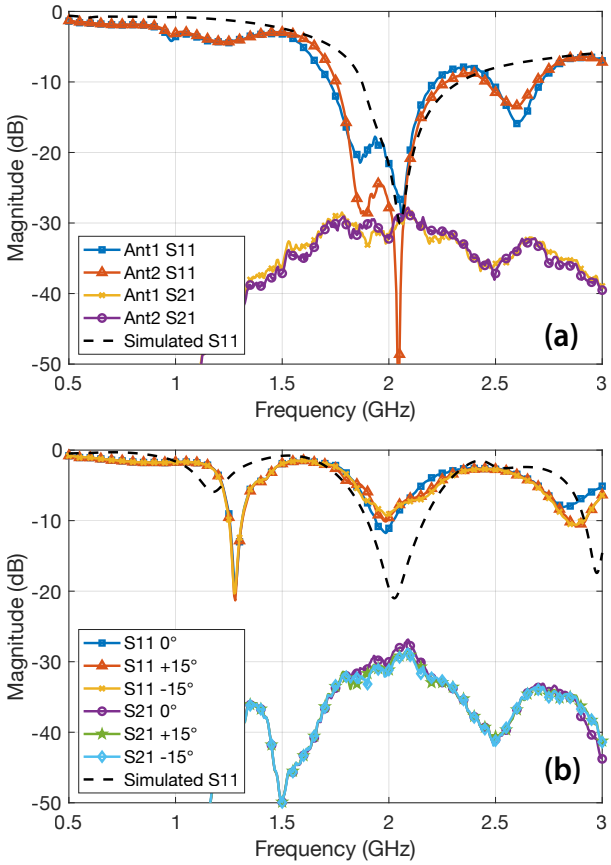

Figure 4.2: S-parameters across frequency for (a) the optimal and (b) proposed array at $\theta = 0°$.

4.2 Results

First, the gain for a reference antenna (G_{REF}) was characterized using measured S-parameters and the three-antenna method [13, 14, 15] at 2.05 GHz. Then, using the same reference antenna, the S-parameters and 1D radiation patterns for the proposed and optimal phased arrays were measured over a $\pm 90°$ range in θ. The measured S-parameters for boresight, $\theta = 0°$, are shown in Fig. 4.2. The S-parameters for the proposed array includes S11 and S21 values for different beam steering directions or beam angles. Note, simulated S11 does not include effect of balun. There is good agreement between the measured and simulated $S11$ parameters and measured S-parameters show clear resonance at the desired RF frequency, 2.05 GHz, providing strong validation for the array design. The $S11$ in the proposed array is reduced compared to the optimal array due to the effects of the parasitic transmission lines shown in Fig. 3.3, which are required to route around the relatively large SMT components.

Second, the radiation patterns for the proposed array ($G_{AUT}(\theta)$) were calculated from

the $S21(\theta)$ data using Eq. 4.1. The Friis free space path loss, L, is 32.15 dB at 2.05 GHz and a distance of 47.2 cm (roughly $3\lambda_{RF}$, since $\lambda_{RF} = 14.6cm$ at 2.05 GHz).

$$G_{AUT}(\theta) = 20\log_{10}(|\boldsymbol{S21(\theta)}|) + L - G_{REF} \tag{4.1}$$

Finally, to calculate the gain for the optimal array, the complex transmission S-parameters measured from each antenna in the optimal array (left and right) are summed with varying degrees of relative phase shift and scaled by $\sqrt{2}$. The gain for each antenna in the optimal phased array, the total gain for the optimal array (steered to a few key angles), and the array gain for the proposed phased array are shown in Fig. 4.3. It can be seen from Fig. 4.3b and Fig. 4.3c that the beam for the optimal and proposed arrays are both steered across a range of beam angles. In the optimal phased array this is done by lossless, high precision, digital phase shifting and combining in post-process. This is analogous to digital beamforming with perfect phase control. While in the proposed phased array, the beam angle is steered by BIPS and TLT-based power combining.

The gains for the optimal and proposed phased array for specific beam angles are compared directly in Fig. 4.4. The results show that we can predictably steer the array's beam using programmable admittances in a series array configuration with minimal loss (1.07 dB) even with very low quality factor (Q_{COMP}) discrete components ($8 > Q_{COMP} > 5$). Because of the large step size of the DTC at 2 GHz (800 pF), only a few beam angles were characterized in these experiments. However, with custom ASIC design it is possible to get much smaller capacitive step sizes and better Q_{COMP}, even at higher frequencies.

The bandwidth for the proposed array was estimated from the frequency-dependent loss, i.e. difference in gain for the proposed and optimal array. By plotting the proposed array's loss versus frequency and noting the frequencies at which there is 3 dB loss, the 3 dB fractional bandwidth was calculated. As shown in Fig. 4.5, the proposed beamformer has a fraction bandwidth of 20.4%.

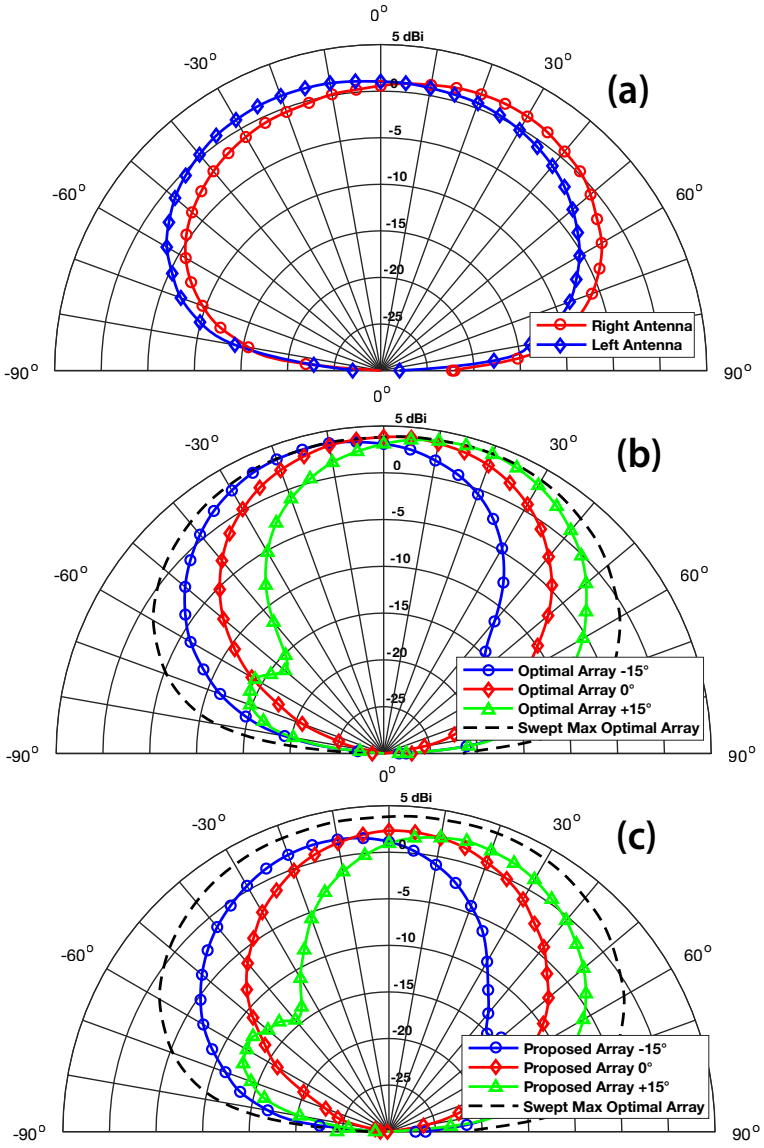

Figure 4.3: (a) Measured gain across azimuth angle, θ, for left and right antenna in optimal phased array. (b) Calculated gain for optimal phased array after post processing to construct the beam from individual antenna gain data. (c) Measured gain across azimuth angle for proposed phased array for different beam angles configurations. The 'Swept Max' refers to maximum gain at each azimuth angle that could be achieved using the optimal phased array and optimal steering.

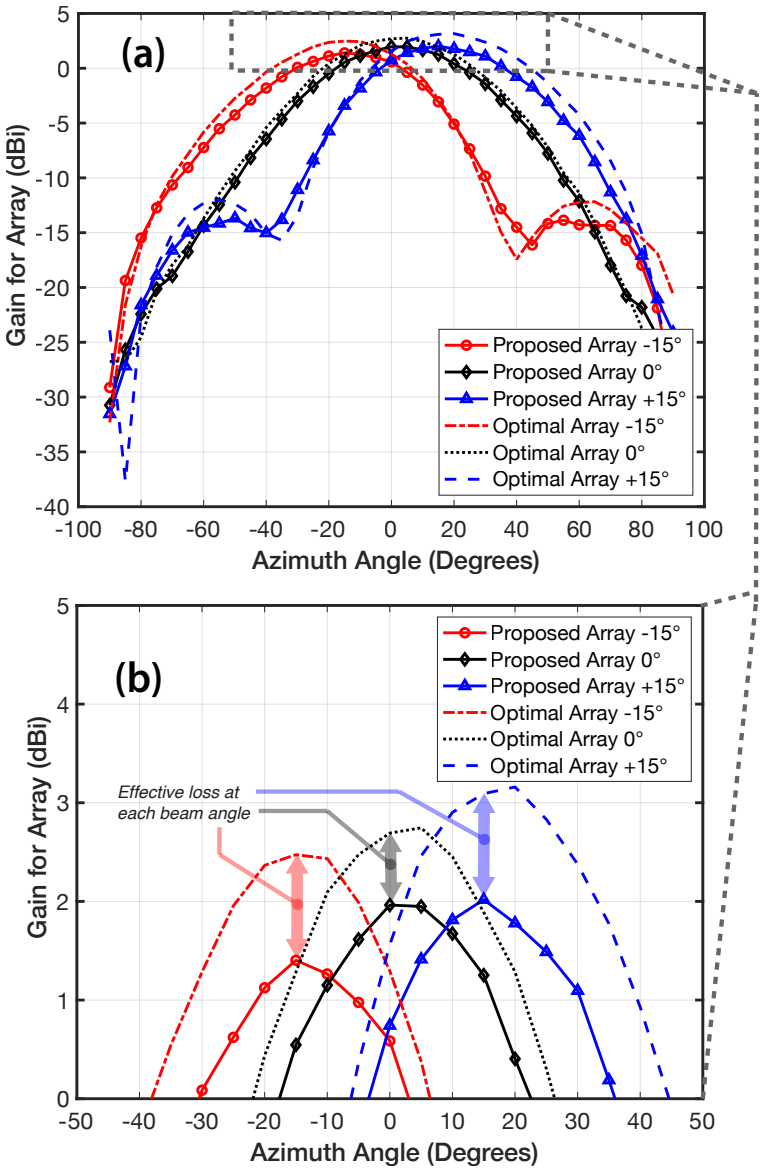

Figure 4.4: Gain for the proposed (solid) and optimal (dashed) phased arrays at $\theta = +15°, 0°, -15°$. (b) Is a subsection of (a) showing the highlighted region in the gray box and emphasizing the effective loss at each beam angle.

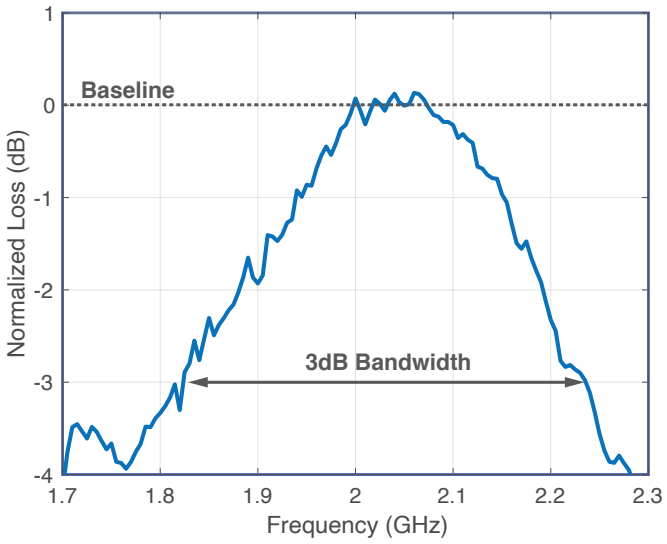

Figure 4.5: Normalized loss over frequency for proposed array showing greater than 20% franctional bandwidth.

Chapter 5

Conclusion

5.1 Summary

This work presents theoretical support, simulation results and experimental validation for a novel, fully-passive, low-loss RF beamforming technique. The technique uses balanced tuning of passive components for low-loss phase shifting and TLT-based power combiners incorporated into the antenna feed lines to avoid additional lossy RF structures for power combining.

To enable experimental validation, a 2-element, dipole array was designed at 2.05 GHz with half-wavelength spacing and tested in both an optimal phased array configuration and the proposed fully-passive RF beamforming configuration. The experimental results showed only a 1.07dB reduction in gain (i.e. loss), when comparing this proposed array to the optimal array. The loss is primarily driven by the common-mode currents in the TLTs and component losses in the tunable passives that implement the phase shifters. This compares well with the typical losses seen in state-of-the-art phase shifters, which are in generally excess of 2 dB [16, 17, 18], and do not include summation losses. The loss of the proposed passive beamformer is compared with commercial beamformer in Table. 5.1.

The proposed balanced-impedance-tuning-based phase shifters have the potnetial for low loss since they have so few lossy components. But because they rely on the direct combination of signals to generate a broadband match, they do not allow for individual-element amplitude

	IL	**Bits**	**Frequency**	**Includes Combiner Loss**
This Work	1.07 dB	1.5	2 GHz	Yes
Miller MM6002 [16]	1.80 dB	3	1-3 GHz	No
Qoevo DA007389 [17]	5.0 dB	6	2.5-4 GHz	No
ADI HMC647ALP6E [18]	4.0 dB	6	2.5-3.1 GHz	No

Table 5.1: Phase shifter comparison table

control. This could prevent the use of complex beamforming algorithms when leveraging this technique.

Overall, good agreement is seen between theoretical, simulation and experimental results, indicating that the proposed beamforming technique is well understood. We believe the current implementation strategies will carry over well to higher frequencies. The phase shifters use a tunable LC tank which has seen broad application at millimeter-wave frequencies. Similarly, the TLTs leverage transmission-line structures which are also common at millimeter-wave frequencies. Furthermore, with reasonable integration (high-Q on-chip passives) the impacts of parasitics could be minimized, providing a path forward for the use of this technique at higher frequencies.

5.2 Future Research

Significant work can be done to better understand and improve this relatively new RF beamforming technique. Below are a few suggested avenues for future research.

Phased arrays are not commonly deployed at 2 GHz because of the large array sizes required and the relatively low path loss. They are more often used at higher frequencies where a larger number of antennas can be combined in the array, while occupying a small footprint [19]. Therefore, for the proposed technique to find application it will be important to demonstrate that it works well at higher frequencies and with larger numbers of antenna elements. It will also be important to find ways to extend the range of the phase shift beyond $\pm 90^\circ$ since many applications find broad ranges of scan angles to be desirable and improve the resolution [19]. In addition, it is important to better understand the theory behind the mechanisms of loss that apply to the proposed technique. It is qualitatively understood that the Z'_{CM} and Q_{COMP} affect the performance of the beamformer but to further optimize the design and integration of the proposed technique, more precise quantitative analysis is required. This will be especially true at higher frequencies and with more antenna elements.

Bibliography

[1] Don Parker and David C Zimmermann. "Phased arrays-part 1: theory and architectures". In: *IEEE Trans. Microw. Theory Techn.* 50.3 (Mar. 2002), pp. 678–687.

[2] Kilian Roth et al. "A comparison of hybrid beamforming and digital beamforming with low-resolution ADCs for multiple users and imperfect CSI". In: *IEEE J. Sel. Topics Signal Process.* 12.3 (Mar. 2018), pp. 484–498.

[3] Han Yan et al. "Performance, power, and area design trade-offs in millimeter-wave transmitter beamforming architectures". In: *IEEE Circuits Syst. Mag.* 19.2 (May 2019), pp. 33–58.

[4] Waqas Bin Abbas, Felipe Gomez-Cuba, and Michele Zorzi. "Millimeter wave receiver efficiency: A comprehensive comparison of beamforming schemes with low resolution ADCs". In: *IEEE Trans. Wireless Commun.* 16.12 (Oct. 2017), pp. 8131–8146.

[5] Kerim Kibaroglu, Mustafa Sayginer, and Gabriel M Rebeiz. "A Low-Cost Scalable 32-Element 28-GHz Phased Array Transceiver for 5G Communication Links Based on a 2×2 Beamformer Flip-Chip Unit Cell". In: *IEEE J. Solid-State Circuits* 53.5 (Jan. 2018), pp. 1260–1274.

[6] Frank Ellinger et al. "Integrated adjustable phase shifters". In: *IEEE Microwave Magazine* 11.6 (2010), pp. 97–108.

[7] Ersch Rotholz. "Transmission-line transformers". In: *IEEE Transactions on Microwave Theory and Techniques* 29.4 (1981), pp. 327–331.

[8] A. M. Niknejad et al. "Integrated circuit transmission-line transformer power combiner for millimetre-wave applications". In: *Electron. Lett.* 43.5 (Mar. 2007), pp. 47–48. ISSN: 0013-5194. DOI: 10.1049/el:20073503.

[9] Umut Kodak and Gabriel M Rebeiz. "Bi-directional flip-chip 28 GHz phased-array core-chip in 45nm CMOS SOI for high-efficiency high-linearity 5G systems". In: *IEEE Radio Freq. Integr. Circuits Symp.* Honolulu, Hawaii, USA, June 2017, pp. 61–64.

[10] Yahya Tousi and Alberto Valdes-Garcia. "A Ka-band digitally-controlled phase shifter with sub-degree phase precision". In: *IEEE Radio Freq. Integr. Circuits Symp.* IEEE. May 2016, pp. 356–359.

[11] Hong-Teuk Kim et al. "A 28-GHz CMOS Direct Conversion Transceiver With Packaged 2×4 Antenna Array for 5G Cellular System". In: *IEEE J. Solid-State Circuits* 53.5 (Jan. 2018), pp. 1245–1259.

[12] M. N. Abdallah et al. "Defining the starting distance for the far field of antennas operating in any environment". In: *2016 IEEE Conference on Antenna Measurements Applications (CAMA)*. 2016, pp. 1–4. DOI: 10.1109/CAMA.2016.7815743.

[13] Y. Huang and K. Boyle. *"Antenna manufacturing and measurements," in Antennas: From Theory to Practice, 1st ed.* Hoboken, NJ, USA: Wiley, 2008, pp. 272–273.

[14] Michael Hillbun. "Practical Antennas: Antenna Measurements". In: *Diamond Engineering* (2010). URL: http://www.diamondeng.net/library/AntennaMeasurement.pdf.

[15] AC Newell and DM Kerns. "Determination of both polarisation and power gain of antennas by a generalised 3-antenna measurement method". In: *Electron. Lett.* 7.3 (Feb. 1971), pp. 68–70.

[16] Miller MMIC LLC. "GaAs pHEMT MMIC 3-bit digital control phase shifter 1-3GHz datasheet". In: V1.0.0 (2017). URL: https://www.millermmic.com/pdf/mmic_digitalcontrolphaseshifter/MM6002.pdf.

[17] Qorvo. "CMD175P4 2-4 GHz (S Band) 5-Bit digital phase shifter MMIC datasheet". In: Rev 1.4 (2018). URL: https://www.qorvo.com/products/d/da007389.

[18] ADI. "HMC647ALP6E GaAs MMIC 6-BIT DIGITAL PHASE SHIFTER, 2.5 - 3.1 GHz datasheet". In: v01.0217 (2022). URL: https://www.analog.com/media/en/technical-documentation/data-sheets/HMC647ALP6E.pdf.

[19] Risto Valkonen. "Compact 28-GHz phased array antenna for 5G access". In: *2018 IEEE/MTT-S International Microwave Symposium - IMS*. 2018, pp. 1334–1337. DOI: 10.1109/MWSYM.2018.8439223.